Hydrothermal synthesis and characterization of monodisperse α-Fe_2O_3 nanocubes

Jing Liu[1], Jie Wang[1], Jincheng Sun[1], Yaru Li[1], Feng Lu[2]

[1]*School of Municipal and Environmental Engineering, Shandong Jianzhu University, Jinan, Shandong 250101, People's Republic of China*
[2]*Institute of Chemical Engineering, Jinan, Shandong 250100, People's Republic of China*
E-mail: liujing99@sdu.edu.cn

Published in Micro & Nano Letters; Received on 25th April 2014; Revised on 30th August 2014; Accepted on 9th September 2014

Monodisperse α-Fe_2O_3 nanocubes with a mean size of 85 nm have been prepared by heating an aqueous solution of iron (III) nitrate in the presence of a certain amount of alkali without any additional organic reagents or templates in a hydrothermal route. The structure and morphology of the products were characterised by X-ray diffraction, transmission electron microscopy and field-emission scanning electron microscopy. The results have shown that the crystal morphology continually changes at higher temperatures and α-FeOOH was generated as the intermediate during the hydrothermal dehydration reaction. In addition, the optimum temperature and reaction time of the hydrothermal synthesis of these α-Fe_2O_3 nanocubes were 200°C and 5 h, respectively.

1. Introduction: Monodisperse nanoparticles have become a new focus of study because of their potential application in optics [1], biomedical sciences [2], catalysis [3] and other fields. In recent years, considerable efforts have been focused on the preparation of monodisperse inorganic nanoparticles [4–8]. For example, Yang's group developed hydrothermal and solvothermal methods to synthesise monodisperse micro and nanoparticles, such as CeO_2 [4], In_2O_3 [5] and $Ni(OH)_2$ [6]. Monodisperse metal nanoparticles with controllable size and different shapes have also been fabricated by many processes [7, 8].

As one of the most important metal oxides, iron oxide nanoparticles have attracted increasing attention owing to their wide applications in catalysis [9], adsorption [10], pollutant removal [11], sensors [12] and batteries [13]. Many researchers have taken advantage of Fe_2O_3 nanoparticles as catalysts of the Fenton oxidation of endocrine disrupting compounds in domestic and industrial wastewater [14, 15]. The synthesised α-Fe_2O_3 nanoparticles in this Letter are applied particularly to photo-assisted Fenton catalytic oxidation. Also, much progress has been made on the preparation of nanostructured α-Fe_2O_3 with various morphologies [16–21], including cubic morphology [22–25]. For instance, Hou *et al.* [23] reported that cubic α-Fe_2O_3 particles could be prepared by hydrothermal synthesis from a solution of urotropine ($(CH_2)_6N_4$) and ferric chloride. α-Fe_2O_3 nanocubes were also fabricated via a hydrothermal route using a small amount of *n*-decanoic acid ($C_9H_{19}COOH$) as the organic surface modifier [24]. However, most previous synthetic methods need toxic organic reagents or multistep post-treatments. The use of organic reagents or templates can introduce impurities and increase preparation costs. In addition, multistep post-treatments can also increase the complexity of the preparation process. The hydrothermal method of this work not only overcame the above drawbacks but also possessed several advantages: (a) better control of the morphology and size of the crystals, (b) easier operation of large-scale production and (c) shorter synthesis time. In this Letter, monodisperse α-Fe_2O_3 nanocubes with uniform sizes of about 85 nm have been fabricated by heating an aqueous solution of iron (III) nitrate in the presence of alkali without any additional templates or surfactants. The whole synthesis process without using any toxic organic reagents or templates can avoid organic pollution of the environment. Reaction temperature had a great influence on the morphology of the α-Fe_2O_3 nanoparticles. α-FeOOH from the dehydration of Fe$(OH)_3$ acted as an intermediate during the preparation of α-Fe_2O_3 nanocubes. Furthermore, the reaction conditions for the synthesis of these α-Fe_2O_3 nanocubes were optimised.

2. Experimental

2.1. Chemicals: For our experiments, iron (III) nitrate (Fe$(NO_3)_3{\cdot}9H_2O$, ≥99.0%), sodium hydroxide (NaOH, ≥99.0%) and ethanol (>99.0%) were purchased from the Sinopharm Chemical Reagent Co. Ltd. Deionised water was used throughout.

2.2. Synthesis: In an optimised synthesis of the monodisperse α-Fe_2O_3 nanocubes, 8.0 ml of 0.60 M $Fe(NO_3)_3$ aqueous solution was added into a Teflon-lined autoclave of 20 ml capacity. Then 8.0 ml of 0.60 M NaOH aqueous solution was added slowly to the autoclave under continuous stirring. After vigorous stirring for 15 min, the iron oxide precursors were obtained and the autoclave was then heated to different temperatures for 7 h. After cooling to room temperature naturally, the red precipitate was collected by centrifugation, washed with deionised water six times, and then with ethanol two times. The final solids were obtained by drying for 3 h at 60°C. To find the best reaction temperature, samples were synthesised at 120, 160 and 200°C (Table 1). To further investigate the effects of reaction time, samples were synthesised at the optimum temperature (200°C) for 5 and 3 h (Table 1).

2.3. Characterisation: The phase purity of the samples was examined by X-ray diffraction (XRD) using a Bruker D8-Advance powder X-ray diffractometer with Cu-Kα radiation ($\lambda = 0.15418$ nm). The morphology and nanostructure of the products were characterised using a transmission electron microscope (TEM, JEM 100-CX II) with an accelerating voltage of 80 kV, and a field-emission scanning electron microscope (FESEM, Hitachi S-4800).

Table 1 Synthesis parameters for different samples

Sample	NaOH, M	Fe^{3+}, M	Hydrothermal temperature, °C	Reaction time, h
1	0.30	0.30	120	7
2	0.30	0.30	160	7
3	0.30	0.30	200	7
4	0.30	0.30	200	5
5	0.30	0.30	200	3

doi: 10.1049/mnl.2014.0212

3. Results and discussion: The XRD patterns of the sample obtained at 200°C for 7 h (Fig. 1*a*) are similar to samples obtained at 120 and 160°C for 7 h (data not shown). The diffraction peaks of all the samples prepared for 7 h can be well indexed to the face-centred cubic phase α-Fe_2O_3 (JCPDS No. 33-0664) without any parasitic secondary phases. The high magnification SEM image of the sample reacted for 7 h at 200°C, shown in Fig. 1*b*, indicates that the particles are cube-like in shape with an average edge length of 85 nm and all these particles are monodisperse particles with narrow size distribution.

To clearly track the crystal growth, the evolution process was monitored and the structures were investigated systematically by TEM. Fig. 2 displays TEM images of samples obtained at 120, 160 and 200°C for 7 h. It is worth noting that when the reaction temperature was 120°C, the formed particles exhibited irregular shapes as shown in Fig. 2*a*. When the reaction temperature was raised to 160°C, many particles agglomerated together to form colloidal particles (Fig. 2*b*). At 200°C, the edges of the particles sharpened to form cubes with an average edge length of 85 nm (Fig. 2*c*).

On the basis of the above results, under hydrothermal conditions the nanocrystals go through several growth stages. In the first stage, irregular-shaped α-Fe_2O_3 nanocrystals with a rough surface were formed; the dispersibility of these particles with uneven sizes was poor (based on the TEM image in Fig. 2*a*). In the second stage, the initially formed nanocrystals agglomerated to form larger colloidal particles to reduce their surface energy. At 160°C, the edges of some particles gradually sharpened to form a nearly cubic morphology, because of further dehydration reactions of the colloidal particles. Upon further increasing the temperature to 200°C, nanocubes with sharp edges predominated in the final product because of the dehydration reaction equilibrium. The TEM image in Fig. 2*c* further confirms their good dispersibility, and the average edge length of the products also increased to about 85 nm. Therefore, reaction temperature has a great influence on the formation of Fe_2O_3 nanocubes and well-defined Fe_2O_3 nanocubes were obtained at 200°C.

The formation mechanism of the synthesised α-Fe_2O_3 nanocubes was investigated using XRD (Figs. 3*a* and *b*). It is worth noting that all the detectable XRD peaks observed after 3 h of reaction at 200°C can be indexed to two phases, α-FeOOH and α-Fe_2O_3, but the relative intensities of the α-FeOOH phase diffraction peaks were weak. However, the XRD patterns of the sample reacted for 5 h at 200°C showed only rather sharp characteristic diffraction peaks of α-Fe_2O_3 (JCPDS Card No. 33-0664) without any parasitic secondary phases of the α-FeOOH phase. As shown above, the characteristic diffraction peaks of α-FeOOH were not found in the XRD patterns of samples obtained at 120, 160 and 200°C for 7 h (Fig. 1*a*). It can be concluded that all α-FeOOH

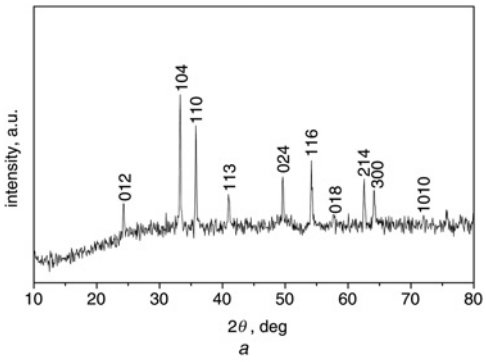

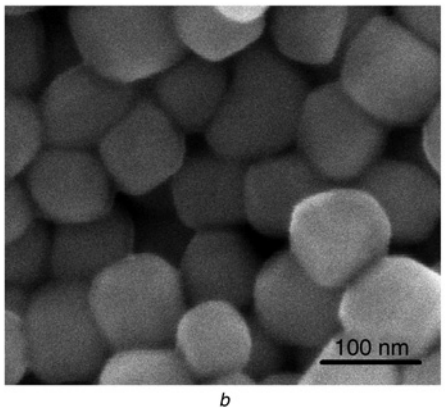

Figure 1 *XRD patterns (Fig. 1a) and SEM images (Fig. 1b) of nanoparticles synthesised at 200°C for 7 h (all XRD peaks can be indexed to α-Fe_2O_3)*

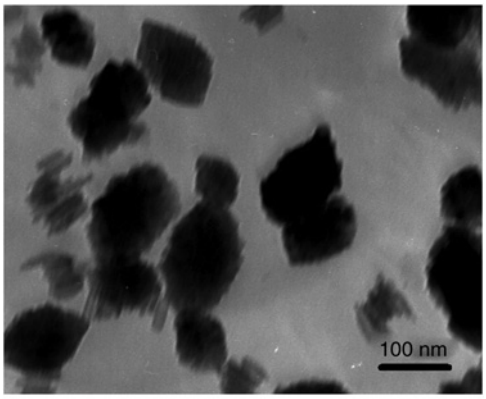

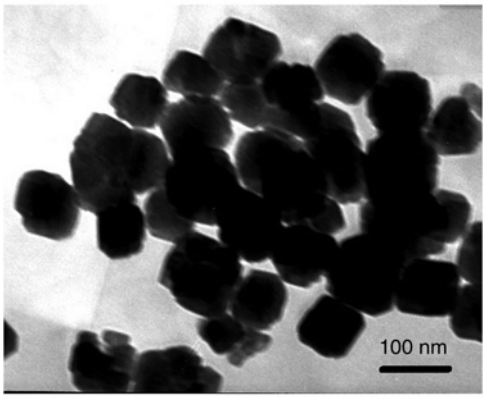

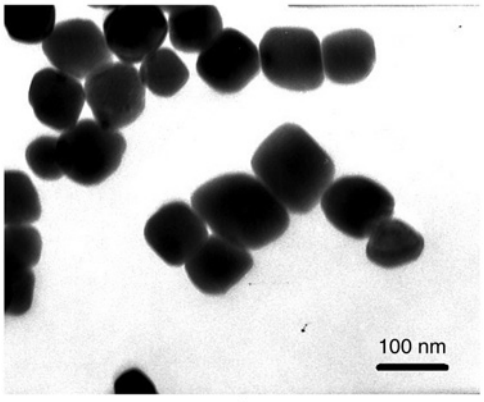

Figure 2 *TEM images of α-Fe_2O_3 nanocubes prepared at different temperatures of 120°C (Fig. 2a), 160°C (Fig. 2b) and 200°C (Fig. 2c) showing increasingly well-defined cubic morphologies*

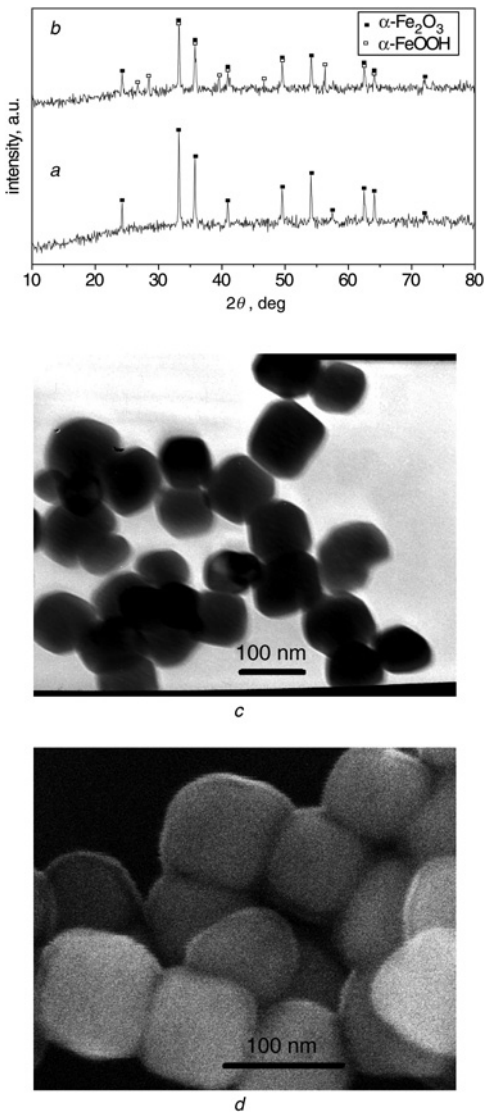

Figure 3 *XRD patterns, TEM and SEM images of samples prepared at 200° C for different times*
a XRD patterns of the 5 h sample
b XRD patterns of the 3 h sample
c TEM images of the 5 h sample
d SEM images of the 5 h sample

particles in the products will disappear when the reaction time exceeds 5 h.

We can conclude from the above results that a great quantity of intermediate, α-FeOOH nanoparticles were formed in the initial stage of the hydrothermal reaction. As the reaction proceeded, the initially formed α-FeOOH nanoparticles tend to further dehydrate and converted to α-Fe_2O_3. Phase pure α-Fe_2O_3 nanocubes were obtained when the dehydration reactions were complete. The equations could be described as follows

$$Fe(NO_3)_3 + 3NaOH \rightarrow Fe(OH)_3 \downarrow + 3NaNO_3 \quad (1)$$

$$Fe(OH)_3 \rightarrow \alpha - FeOOH + H_2O \quad (2)$$

$$2\alpha - FeOOH + 0.5O_2 \rightarrow \alpha - Fe_2O_3 + 2OH^- \quad (3)$$

During the reaction, the oxidising atmosphere created by the oxidant $NaNO_3$, protected the Fe^{3+} ions from being reduced. In addition, the solubility of α-FeOOH is lower than that of Fe $(OH)_3$, and the solubility of α-Fe_2O_3 is even lower than α-FeOOH. Very high supersaturation can be achieved in this process because of the very low solubility of α-FeOOH and α-Fe_2O_3, therefore very fine nanocrystals are obtained [26]. The TEM and SEM images of sample 4 (Figs. 3*c* and *d*) showed that the edges of particles had also sharpened to form cubes. From the product morphologies and phase characterisation, we can assert that 5 h of reaction time is sufficient. However, the detailed mechanism of the formation of monodisperse α-Fe_2O_3 nanocubes needs to be further explored.

4. Conclusions: We have demonstrated a facile approach to the synthesis of monodisperse α-Fe_2O_3 nanocubes with a mean size of 85 nm. Obvious shape changes from irregular to cubic nanoparticles can be achieved by raising the temperature to 200° C in this hydrothermal process. The XRD results indicated that α-FeOOH was formed as an intermediate in the hydrothermal synthesis process. The optimum temperature and reaction time of this hydrothermal route were 200°C and 5 h, respectively.

5. Acknowledgments: This work was supported by the Science and Technology Project of Shandong colleges (Grant no. J11LB18). The authors thank Dr. Pamela Holt, Shandong University, for proofreading the manuscript.

6 References

[1] Hubenthal F.: '1.13-noble metal nanoparticles: synthesis and optical properties', *Comprehen. Nanosci. Technol.*, 2011, **1**, pp. 375–435
[2] Xu C.J., Sun S.H.: 'New forms of superparamagnetic nanoparticles for biomedical applications', *Adv. Drug Deliv. Rev.*, 2013, **65**, pp. 732–743
[3] Feng X., Mao G.Y., Bu F.X., *ET AL.*: 'Controlled synthesis of monodisperse $CoFe_2O_4$ nanoparticles by the phase transfer method and their catalytic activity on methylene blue discoloration with H_2O_2', *J. Magn. Magn. Mater.*, 2013, **343**, pp. 126–132
[4] Yang Z.J., Yang Y.Z., Liang H., Liu L.: 'Hydrothermal synthesis of monodisperse CeO_2 nanocubes', *Mater. Lett.*, 2009, **63**, pp. 1774–1777
[5] Yang H.X., Yang Z.J., Liang H., *ET AL.*: 'Solvothermal synthesis of In $(OH)_3$ nanorods and their conversion to In_2O_3', *Mater. Lett.*, 2010, **64**, pp. 1418–1420
[6] Liang H., Yang H.X., Liu L., Yang Z.J., Yang Y.Z.: 'Fabrication of porous α-$Ni(OH)_2$ microflowers by a facile template-free method', *Superlatt. Microstr.*, 2010, **48**, pp. 569–576
[7] Kwon K., Lee K.Y., Kim M., *ET AL.*: 'High-yield synthesis of monodisperse polyhedral gold nanoparticles with controllable size and their surface-enhanced Raman scattering activity', *Chem. Phys. Lett.*, 2006, **432**, pp. 209–212
[8] Kawasaki S.I., Xiuyi Y., Sue K., *ET AL.*: 'Continuous supercritical hydrothermal synthesis of controlled size and highly crystalline anatase TiO_2 nanoparticles', *J. Supercrit. Fluids*, 2009, **50**, pp. 276–282
[9] Sakthivel S., Geissen S.-U., Bahnemann D.W., Murugesan V., Vogelpohl A.: 'Enhancement of photocatalytic activity by semiconductor heterojunctions: α-Fe_2O_3, WO_3 and CdS deposited on ZnO', *J. Photochem. Photobiol. A, Chem.*, 2002, **148**, pp. 283–293
[10] Salih H.H., Patterson C.L., Sorial G.A., *ET AL.*: 'The implication of iron oxide nanoparticles on the removal of trichloroethylene by adsorption', *Chem. Eng. J.*, 2012, **193–194**, pp. 422–428
[11] Wang N., Zhu L.H., Wang D.L., *ET AL.*: 'Sono-assisted preparation of highly-efficient peroxidase-like Fe_3O_4 magnetic nanoparticles for catalytic removal of organic pollutants with H_2O_2', *Ultrason. Sonochem.*, 2010, **17**, pp. 526–533
[12] Umar A., Akhtar M.S., Dar G.N., Baskoutas S.: 'Low-temperature synthesis of α-Fe_2O_3 hexagonal nanoparticles for environmental remediation and smart sensor applications', *Talanta*, 2013, **116**, pp. 1060–1066
[13] Reddy M.V., Yu T., Sow C.H., *ET AL.*: 'α-Fe_2O_3 nanoflakes as an anode material for Li-ion batteries', *Adv. Funct. Mater.*, 2007, **17**, pp. 2792–2799

doi: 10.1049/mnl.2014.0212

[14] Cong Y.Q., Li Z., Zhang Y., Wang Q., Xu Q.: 'Synthesis of α-Fe_2O_3/TiO_2 nanotube arrays for photoelectro-Fenton degradation of phenol', *Chem. Eng. J.*, 2012, **191**, pp. 356–363
[15] Zelmanov G., Semiat R.: 'Iron(3) oxide-based nanoparticles as catalysts in advanced organic aqueous oxidation', *Water Res.*, 2008, **42**, pp. 492–498
[16] Jiao H., Wang J.L.: 'Single crystal ellipsoidal and spherical particles of α-Fe_2O_3: hydrothermal synthesis, formation mechanism, and magnetic properties', *J. Alloys Compd.*, 2013, **577**, pp. 402–408
[17] Song L.M., Zhang S.J., Chen B., Ge J.J., Jia X.C.: 'A hydrothermal method for preparation of α-Fe_2O_3 nanotubes and their catalytic performance for thermal decomposition of ammonium perchlorate', *Colloids. Surf. A, Physicochem. Eng. Aspects*, 2010, **360**, pp. 1–5
[18] Peng D.F., Beysen S., Li Q., Sun Y.F., Yang L.Y.: 'Hydrothermal synthesis of monodisperse α-Fe_2O_3 hexagonal platelets', *Particuology*, 2010, **8**, pp. 386–389
[19] Mohammadikish M.: 'Hydrothermal synthesis, characterization and optical properties of ellipsoid shape α-Fe_2O_3 nanocrystals', *Ceram. Int.*, 2014, **40**, pp. 1351–1358
[20] Giri S., Samanta S., Maji S., Ganguli S., Bhaumik A.: 'Magnetic properties of α-Fe_2O_3 nanoparticle synthesized by a new hydrothermal method', *J. Magn. Magn. Mater.*, 2005, **285**, pp. 296–302
[21] Woo K., Lee H.J., Ahn J.P., Park Y.S.: 'Sol–gel mediated synthesis of Fe_2O_3 nanorods', *Adv. Mater.*, 2003, **15**, pp. 1761–1764
[22] Zhang X., Niu Y.A., Li Y., *ET AL.*: 'Synthesis, optical and magnetic properties of α-Fe_2O_3 nanoparticles with various shapes', *Mater. Lett.*, 2013, **99**, pp. 111–114
[23] Hou B., Wu Y.S., Wu L.L., *ET AL.*: 'Hydrothermal synthesis of cubic ferric oxide particles', *Mater. Lett.*, 2006, **60**, pp. 3188–3191
[24] Takami S., Sato T., Mousavand T., *ET AL.*: 'Hydrothermal synthesis of surface-modified iron oxide nanoparticles', *Mater. Lett.*, 2007, **61**, pp. 4769–4772
[25] Yin C.Y., Minakshi M., Ralph D.E., *ET AL.*: 'Hydrothermal synthesis of cubic α-Fe_2O_3 microparticles using glycine: surface characterization, reaction mechanism and electrochemical activity', *J. Alloys Compd.*, 2011, **509**, pp. 9821–9825
[26] Teja A.S., Koh P.Y.: 'Synthesis, properties, and applications of magnetic iron oxide nanoparticles', *Prog. Crystal Growth. Character. Mater.*, 2009, **55**, pp. 22–45